SAND96-2861C
CONF-961040--13 SAND--96-2861C

CORROSION OF CURRENT-COLLECTOR MATERIALS IN LI-ION CELLS

Jeffrey Braithwaite, Ganesan Nagasubramanian,
Angelo Gonzales, Samuel Lucero, Wendy Cieslak

Sandia National Laboratories
Albuquerque, NM 87185-0340

ABSTRACT

The primary current-collector materials being used in lithium-ion cells are susceptible to environmental degradation: aluminum to pitting corrosion and copper to environmentally assisted cracking. Pitting occurs at the highly oxidizing potentials associated with the positive-electrode charge condition. However, the pitting mechanism is more complex than that typically observed in aqueous systems in that the pits are filled with a mixed metal/oxide product and exist as mounds or nodules on the surface. Electrochemical impedance was shown to be an effective analytical tool for quantification and verification of visual observations and trends. Two fluorocarbon-based coatings were shown to improve the resistance of Al to localized pitting. Finally, environmental cracking of copper can occur at or near the lithium potential and only if specific metallurgical conditions exist (work hardening and large grain size).

INTRODUCTION

Advanced rechargeable lithium-ion batteries are presently being developed and commercialized worldwide for use in consumer electronic and electric vehicle applications. The motivation behind these efforts involves a favorable combination of energy and power density, service life, cost, and safety. High interest also exists for the specialized low-volume applications (e.g., military and aerospace) where higher reliability and possibly longer service life will be required. Long-term chemical degradation of the cell hardware materials can adversely affect electrical performance, life, and/or safety through increased electrical resistance or even loss of continuity, production of corrosion products that attack or passivate the active materials, introduction of contaminants that also react with active materials (due to loss of hermeticity), and loss of electrolyte. Typically, consumer battery technologies are re-engineered after these secondary types of materials problems become identified.

Potentially serious corrosion problems (current collectors, containers, seals) have been observed in primary lithium batteries. For example, environmentally assisted cracking

This work was supported by the United States Department of Energy under Contract DE-AC04-94AL85000. Sandia is a multiprogram laboratory operated by Sandia Corporation, a Lockheed Martin Company, for the United States Department of Energy.

DISCLAIMER

(EAC) occurs at highly stressed portions of the nickel anode current collector grid in $Li/SOCl_2$ cells, an effect related to alkali-metal embrittlement [1]. Because similar degradation mechanisms may be encountered in the emerging rechargeable lithium-ion battery technology, a dedicated study is being performed to determine if reliability and service life will be compromised by environmental degradation of the materials of construction. The portion of the work that is described in this paper involved an identification of the major materials degradation issues, with the focus on corrosion of the aluminum positive current collector and EAC of the copper negative current collector. A comprehensive report on this study is currently in preparation.

EXPERIMENTAL

Corrosion of aluminum alloys 1100 and 1145 was studied in flooded half-cells that had a standard 3-electrode configuration with a lithium metal as the reference electrode (Figure 1). Two electrolyte formulations were used that nominally represented those originally developed by Sony and Bellcore respectively: 1M $LiPF_6$ in either a 1:1 solvent mixture of propylene carbonate and diethylene carbonate (PC:DEC) or in a 1:1 solvent mixture of ethylene carbonate and dimethyl carbonate (EC:DMC). The solvents were purchased from Mitsubishi Chemical and have a maximum water content of 10 ppm. Individual cells were aged using a simulated low-earth-orbit (LEO) cycle. Each LEO cycle regime consisted of four phases: discharge, constant current charge to voltage cutoff, potentiostatic charge at the voltage cutoff, and dwell (Figure 2). This type of aging simulated the electrical cycling a high-reliability battery in an aerospace application might undergo. The relatively high top-of-charge voltage (4.2 v) was selected as a slight overtest condition (e.g., top-of-charge voltage for a Sony cells is nominally 4.1 V). The test matrix included two forms of a carbon/fluorocarbon-based coating. This coating was applied by air-brushing. The first condition involved curing the coating for 15 minutes at 120°C (final thickness of about 13 μm). A second coating version involved a similar cure followed by polymerization at 232°C for 10 minutes (final thickness of 15 μm).

Aluminum corrosion kinetics and passivation behavior were evaluated using electrochemical impedance spectroscopy (EIS) as a function of cycling, polarization potential (open circuit and 4.2 V vs. Li), temperature (ambient, 35°C, 50°C), and initial water content (as received, + 20 ppm). The relevant electrochemical reactions were modeled using the simplified equivalent electrical circuit shown in Figure 3 (a coating in series with an oxide layer). To obtain reasonable empirical correlations, distributed elements (>>) were substituted for the discrete capacitors used in more general models. Although a distributed element has no physical basis, it behaves mathematically like a "leaky" capacitor. For the bare aluminum electrodes, the coating R-C circuit is simply ignored. Similar experience with aqueous systems has shown that the pitting resistance, R_{pit}, is a reasonable figure-of-merit for the susceptibility of aluminum to pitting corrosion. A lower value describes a greater susceptibility. This parameter, along with the other elements in the equivalent circuit, are calculated from the EIS response.

The susceptibility of copper alloy 110 to EAC was assessed with constant extension rate testing (CERT) and exposure of U-bend samples (with actual tab and grid stock) in flooded cells. Finally, the general observations and trends were validated with post-test analysis of LEO-cycled commercial Sony cells.

RESULTS AND DISCUSSION

Pitting Corrosion of Aluminum

During electrical cycling, the aluminum current collector undergoes a form of pitting corrosion. After several days of cycling (40 LEO cycles), some general attack of the aluminum surface was visible in that an almost electropolished appearance existed, but more importantly, some scattered pitting had initiated (compare Figure 4 and Figure 5). With continued cycling, the pit density increased, as shown in Figure 6 for 690 LEO cycles in the PC:DEC electrolyte. Cycling in the EC:DMC electrolyte resulted in a higher pit density, as shown in Figure 7 for 150 LEO cycles. Curiously, what optically looked like pits after extended cycling in both electrolytes are actually mounds. Based on cross-sectional SEM examination of the foil (as in Figure 8), these mounds appear to be filled in pits. XPS and Auger analyses are presently being performed to help understand this phenomenon. Initial results indicate that the mounds contain both Al^0 and Al_2O_3. Because of the primarily anodic conditions during LEO cycling, the existence of metallic aluminum implies that the mounds are electrically isolated from the foil. Two possible explanations are that 1) corrosion undermined the initial pit and caused the metal to bulge and break away, or 2) metal was redeposited on poorly conductive corrosion products during the discharge portion of the LEO cycle during which cathodic conditions exist (open circuit voltage for Al is between 3.2 and 3.6 V).

The impedance spectroscopy results provide further validation and quantification of the visual observations described above for aluminum pitting. First, as demonstrated in the previous microphotographs, the pit density is higher in the EC:DMC electrolyte. The EIS results show that the EC:DMC electrolyte is more corrosive (lower R_{pit}) than the PC:DEC electrolyte over the majority of the tested cycle life. At cycle 100, the diameter of the semicircular component in Figure 9 that corresponds to R_{pit} is much smaller and, as shown in Figure 10, a distinct separation in R_{pit} exists over the first several hundred cycles. Second, and importantly, the pitting resistance appears to improve with cycling in both electrolytes, but especially EC:DMC. However, as discussed below, this does not imply that the pitting process is self-limiting in either electrolyte. Also note that no attempt was made to analyze impurities and then monitor changes during cycling in either electrolyte. Preliminary surface spectroscopy results indicate that the EC:DMC electrolyte used in this study may have had a higher chloride concentration, which is known to cause pitting corrosion in organic electrolytes [2].

General effects of other environmental parameters are summarized as follows:

- Pitting resistance decreases with increasing applied anodic voltage, a result consistent with the DC polarization behavior (Figure 11).

- Metallurgical purity of the electrode material (alloy 1145 vs. 1100) does not have a substantial effect on pitting behavior (Figure 12).

- The addition of 20 ppm water to the PC:DEC electrolyte appears to substantially improve corrosion resistance (Figure 13). A similar beneficial effect of water (although at much higher levels) has been observed in other related work (PC-stainless steel) and was attributed to a stabilizing effect on the passive layer [3]. More detailed study is needed before a definitive conclusion can be reached.

- The fluoro-carbon based coatings improve corrosion resistance. Figure 14 is a Bode phase plot showing that the uncoated electrode has a single dominant process (represented with a single capacitive/resistive combination and thus one pseudo-time constant), whereas the two coated electrodes show two processes: the non-polymerized with two overlapping time constants, and the polymerized with two distinct time constants. Quantitative modeling of the EIS data is thus a necessary activity to determine the pitting resistance portion of the total EIS resistance. Results indicate that pitting resistance can increase by close to one order of magnitude for coated electrodes. The corresponding increase in resistance was confirmed by a lack of pitting observed on one of the samples (Figure 15) after 445 LEO cycles in the PC:DEC electrolyte. Although not substantiated with surface analysis, a possible reason that these coatings improve the corrosion resistance of aluminum is that much of the active pit area becomes sealed. However, some interaction (swelling and delamination) did occur between the electrolyte and both coatings (Figure 16). As such, the ability to provide long-term protection is unknown.

A final practical validation of these results comes from a section of a positive electrode taken from a commercial Sony Li-Ion cell (1991 vintage) that had been subjected to about 4000 LEO cycles. A representative photomicrograph is shown in Figure 17. Significant localized pitting corrosion of the aluminum occurred to the point that the foil had a large number of visible perforations. Whether or not the holes were at some time mounds is presently unknown because of the difficult nature of removing the active materials without physical disruption of the surface. However, this does prove that the pitting process is not self-limiting. An assessment of the final resistivity of the foil has not been made to determine if the limited general corrosion had a significant effect on cell resistance.

Environmentally Assisted Cracking of Copper

CERT revealed intergranular EAC of copper in large-grained, work-hardened material when tested at an applied voltage of 0V vs. Li/Li^+ (Figure 18). Lack of either of the two metallurgical factors was sufficient to eliminate EAC susceptibility in these tests. For example, the very ductile behavior of fine-grained, work-hardened material under the same electrochemical conditions is shown in Figure 19. The susceptibility conditions are consistent with those observed for Ni in $Li/SOCl_2$ cells [1], implying that the Cu EAC phenomenon is mechanistically similar, that is, Li-induced EAC.

Because the conditions of CERT are so severe, intergranular cracking occurred despite an unfavorable orientation of the grains that were longitutudinally enlongated in the rod (Figure 20). An important effort to complete in the future will be to characterize the range of actual conditions that cause a susceptibility using u-bend samples of varying orientation and stress levels under various simulating cell environments. To date, EAC from the limited u-bend tests completed or from actual foil from commercial cells has not been observed.

REFERENCES

1. J. R. Scully, et.al., *Journal of the Electrochemical Society*, 138, 2229, 1995
2. W.B. Ebner and W.C. Merz, *Proceedings of the 29th Power Sources Symposium*, The Electrochemical Society, p. 265-280, June 1980
3. D.A. Shifler, et.al., *Electrochimica Acta*, 40 (7), 897-905, 1995

ACKNOWLEDGMENT

This work was supported by the United States Department of Energy under Contract DE-AC04-94AL85000. Sandia is a multiprogram laboratory operated by Sandia Corporation, a Lockheed Martin Company, for the United States Department of Energy. The authors would also like to thank Rudy Buchheit and Rob Sorensen for their significant help with the experimental setup and the interpretation of corrosion data.

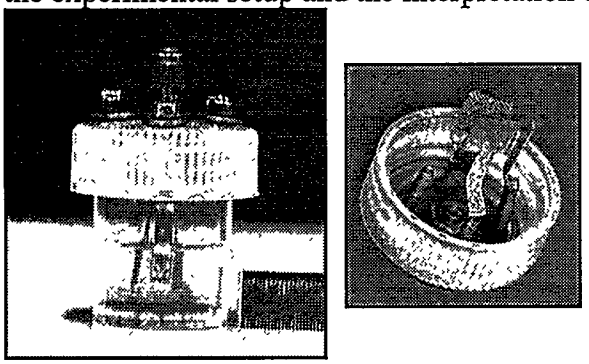

Figure 1. Photographs of the experimental flooded half-cell configuration

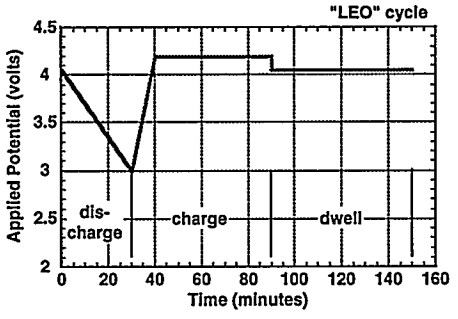

Figure 2. Simulated low-earth-orbit (LEO) electrical cycle regime for Al.

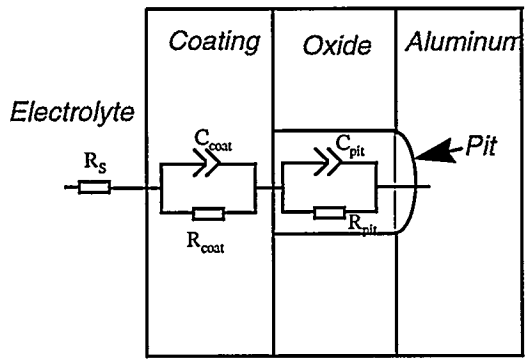

Figure 3. Simplified equivalent electrical circuit for coated aluminum

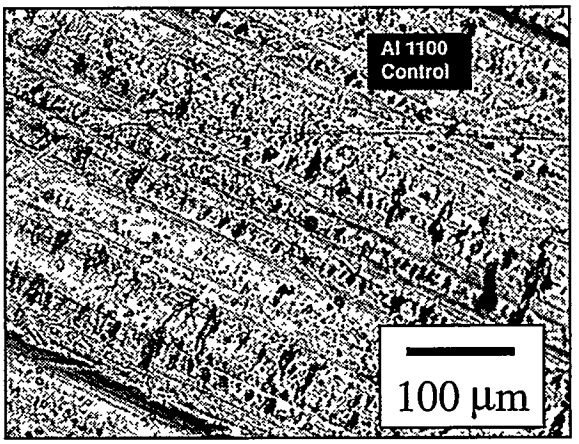

Figure 4. Photograph of the bare Al surface prior to LEO cycling

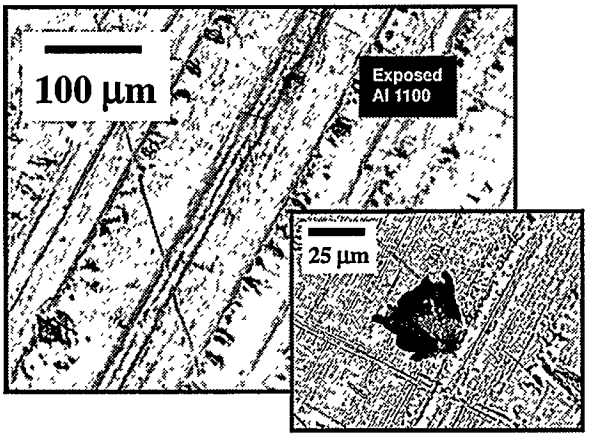

Figure 5. Photographs of the Al surface after 40 LEO cycles in PC:DEC electrolyte

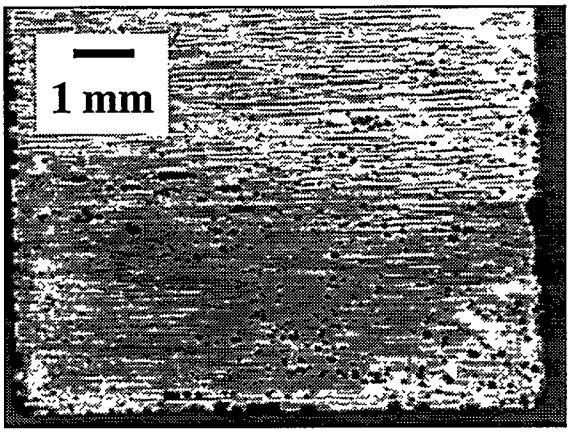

Figure 6. Photograph of an Al surface after 690 LEO cycles in PC:DEC electrolyte

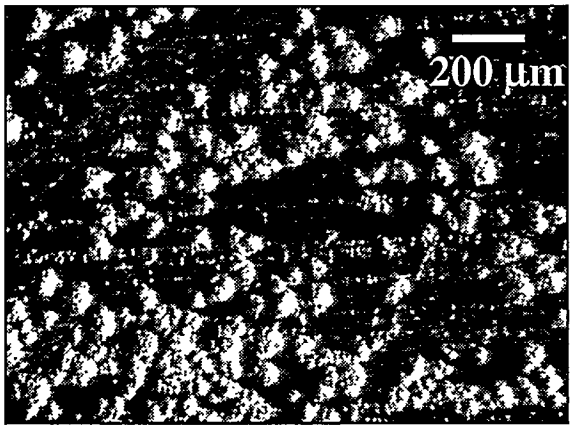

Figure 7. Photographs of the Al surface after 150 LEO cycles in EC:DMC electrolyte

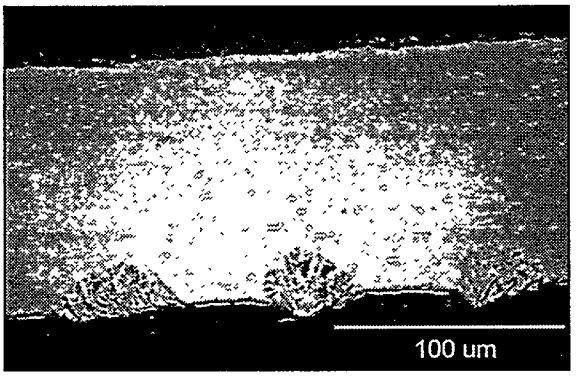

Figure 8. SEM cross-section of Al foil after 150 cycles in EC:DMC electrolyte

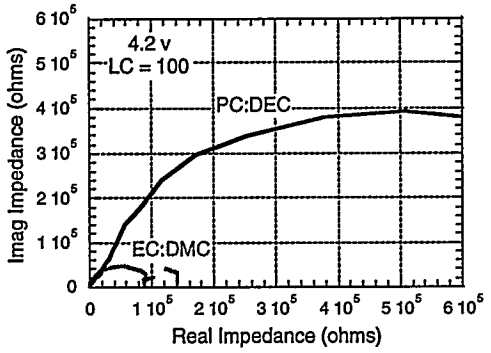

Figure 9. Nyquist plot for Al alloy 1100 in PC:DEC and EC:DMC electrolytes

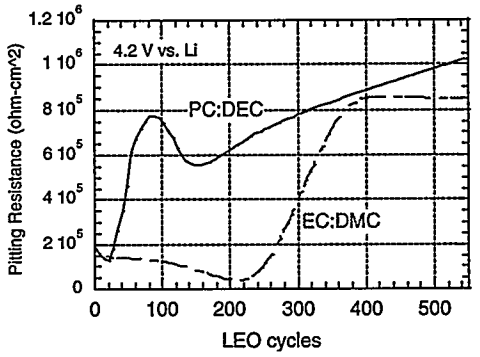

Figure 10. Effect of cycling on the calculated R_{pit} parameter for two electrolytes

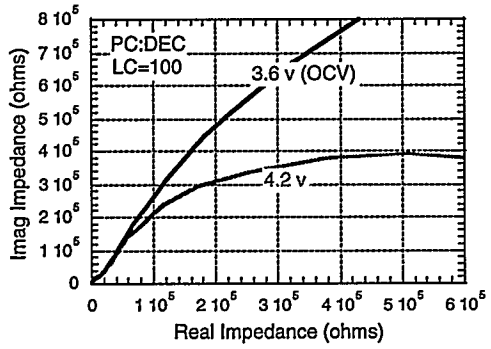

Figure 11. Nyquist plot for aluminum alloy 1100 in PC:DEC electrolyte at 2 voltages

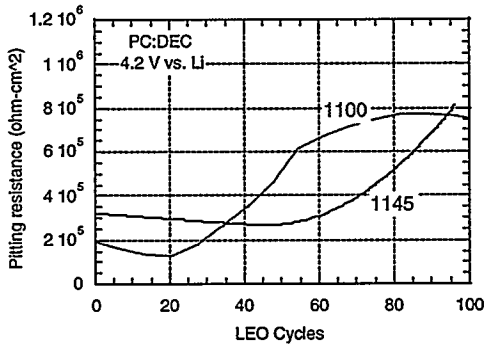

Figure 12. Effect of alloy composition on the calculated R_{pit} parameter

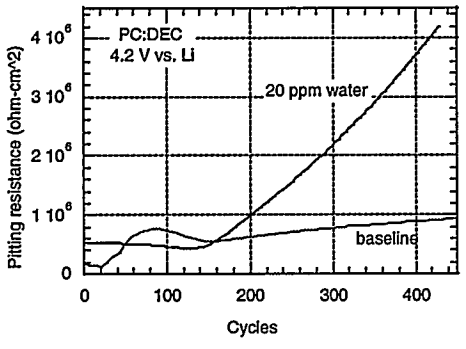

Figure 13. Effect of added water on the calculated R_{pit} parameter

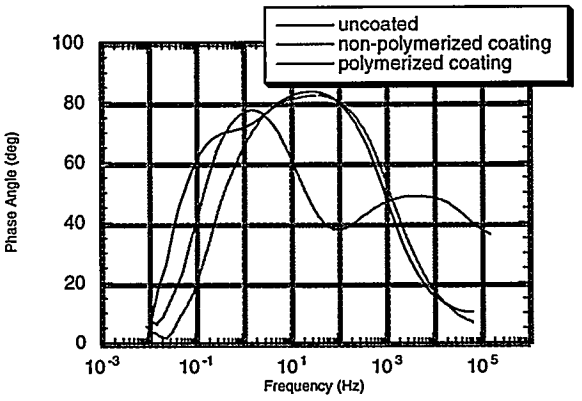

Figure 14. Bode phase plot for uncoated and coated aluminum electrodes

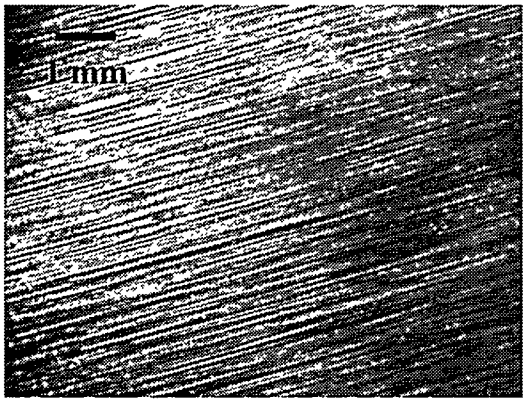

Figure 15. Al substrate after polymerized C coating removed after 445 cycles

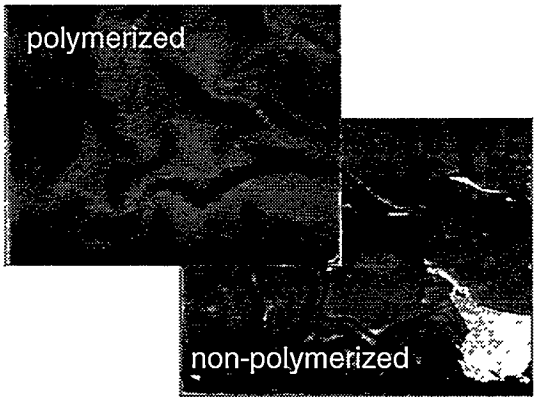

Figure 16. Polymerized and non-polymerized coatings after 445 LEO cycles

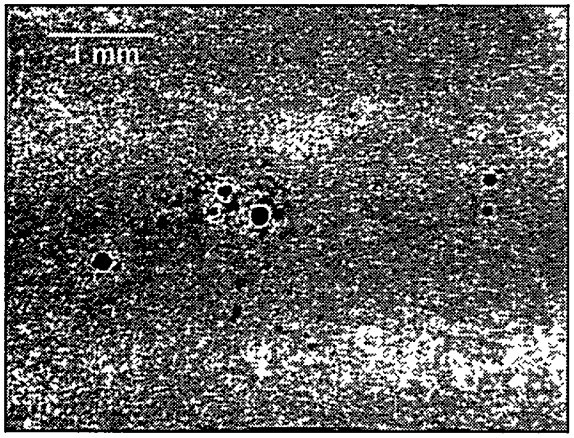

Figure 17. Al current collector from Sony cell after 4000 LEO cycles

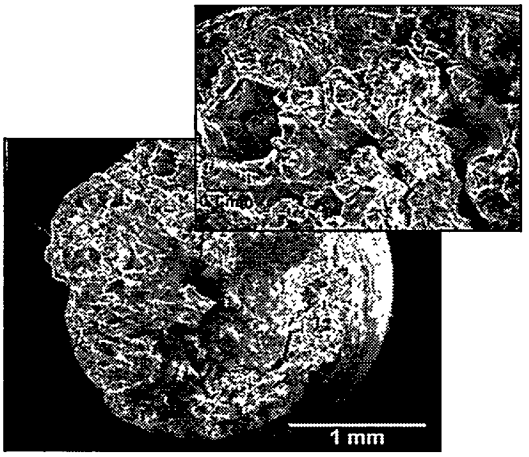

Figure 18. SEM photograph of the brittle fracture surface of coarse-grained, work-hardened copper

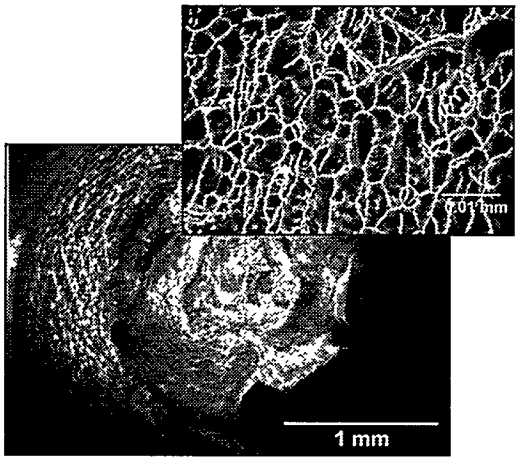

Figure 19. SEM photograph of the ductile fracture surface of fine-grained, work-hardened copper

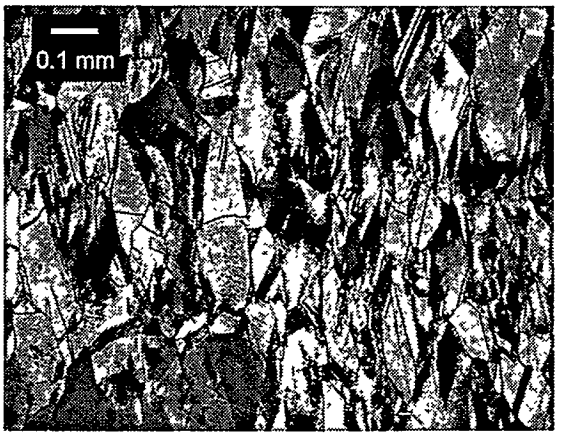

Figure 20. Longitudinal cross-sectioned copper tensile bar that had brittle behavior